Imine Hydrogenation by Tribenzylphosphine Rhodium and Iridium Complexes

Vanessa R. Landaeta,[†,‡] Bianca K. Muñoz,[†,§] Maurizio Peruzzini,*[,‡] Verónica Herrera,[†] Claudio Bianchini,*[,‡] and Roberto A. Sánchez-Delgado*[,†,⊥]

Instituto Venezolano de Investigaciones Científicas (IVIC), Centro de Química, Apartado 21827, Caracas, 1020-A, Venezuela, Istituto di Chimica dei Composti Organometallici (ICCOM-CNR), Via Madonna del Piano 10, Polo Scientifico, 50019, Sesto Fiorentino (FI), Italy, Departament de Química Física i Inorgánica, Universitat Rovira i Virgili, Marcel.lí Domingo, s/n, 43007 Tarragona, Spain, and Chemistry Department, Brooklyn College of the City University of New York, Brooklyn, New York 11210

Received June 14, 2005

The iridium complexes $[Ir(PBz_3)_2(COD)]PF_6$ and $[Ir(py)(PBz_3)(COD)]PF_6$ are effective catalyst precursors for the homogeneous hydrogenation of *N*-(*β*-naphthylmethylene)aniline (N*β*NA) to naphthalene-2-ylmethylphenylamine (PBz_3 = tribenzylphosphine; COD = 1,5-cyclooctadiene; py = pyridine). For comparative purposes, other iridium and rhodium catalysts modified with either PBz_3 or PPh_3 have been tested as catalysts for N*β*NA hydrogenation. A kinetic study of this reaction catalyzed by $[Ir(PBz_3)_2(COD)]PF_6$, $[Ir(py)(PBz_3)(COD)]PF_6$, and $[Rh(PPh_3)_2(COD)]PF_6$, together with in situ NMR experiments, has led us to propose catalytic cycles for the three precursors.

Introduction

The catalytic hydrogenation of imines is of importance in connection with the industrial production of agrochemicals and pharmaceuticals, and it continues to attract much academic interest.[1] Although imines are more refractory than olefins to undergo hydrogenation,[2−4] a number of metal complexes[2] including rhodium[3] and iridium systems[4] have been reported to effectively catalyze the reduction of imines to amines. However, the catalytic mechanisms have not yet been completely understood;[5,6] in particular, few studies are available on the kinetics of imine hydrogenation,[5,6] so that many postulated catalytic cycles are still biased by a high degree of speculation or are assumed to follow simple extensions of known C=C bond hydrogenation pathways.

Scheme 1

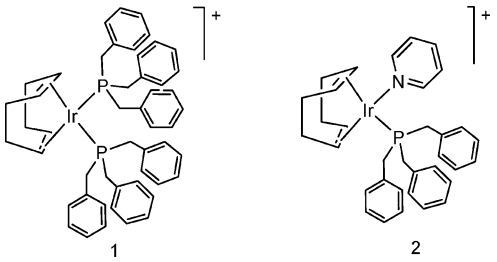

1 2

In a preceding paper, we have reported the synthesis of some iridium complexes stabilized by tribenzylphosphine (PBz_3).[7] These may contain either two *cis*-PBz_3 ligands as in $[Ir(PBz_3)_2(COD)]PF_6$ (**1**) or one PBz_3 ligand as in $[Ir(py)(PBz_3)(COD)]PF_6$ (**2**) (Scheme 1).[7]

An in-depth study of the chemistry of the bis-PBz_3 complex **1**, with particular regard to its reactivity toward H_2, was carried out; the most relevant results are summarized in Scheme 2. The hydrogenation of **1** in coordinating solvents (THF, acetone, or acetonitrile) afforded isolable Ir^{III} bis-solvento trans-dihydrides. Notably, the Ir complex **1** underwent *ortho*-metalation of a benzylic phenyl at room temperature to produce an octahedral Ir^{III} complex with a hydride ligand trans to the *o*-metalated phosphine as the kinetic product. This complex converted to the thermodynamic isomer containing two trans P atoms at room temperature. Similarly, the hydrogenation of the pyridine adduct **2** in coordinating solvents gave bis-solvento dihydrides $[Ir(H)_2(S)_2(py)(PBz_3)]PF_6$, which were identified by in situ NMR

* Corresponding authors. E-mail: claudio.bianchini@iccom.cnr.it; mperuzzini@iccom.cnr.it; Rsdelgado@brooklyn.cuny.edu.

† IVIC.

‡ ICCOM-CNR.

§ Universitat Rovira i Virgili.

⊥ Brooklyn College of the City University of New York.

(1) Carey, F. A.; Sundberg, R. J. *Advanced Organic Chemistry*, 3rd ed.; *Reactions and Synthesis*; Plenum Press: New York, 1990; Part B, p 232.

(2) For leading references on imine hydrogenation, see: (b) Cullen, W.; Fryzuk, M.; James, B. R.; Kutney, J.; Kang, G.; Herb, G.; Thorburn, I.; Spogliarich, R. *J. Mol. Catal.* **1990**, *62*, 243. (f) Bedford, R.; Chaloner, P.; Claver, C.; Fernández, E.; Hitchcock, P.; Ruiz, A. *Chem. Ind.* **1994**, *62*, 181. (g) Willoughby, C.; Buchwald, S. *J. Am. Chem. Soc.* **1994**, *116*, 11703. (i) Uematsu, N.; Fujii, A.; Hashiguchi, S.; Ikariya, T.; Noyori, R. *J. Am. Chem. Soc.* **1996**, *118*, 4916 (k) James, B. R. *Catal. Today* **1997**, *37*, 209. (l) Blaser, H.-U.; Malan, C.; Pugin, B.; Spindler, F.; Steiner, H.; Studer, M. *Adv. Synth. Catal.* **2003**, *345*, 103, and references therein.

(3) Examples of rhodium-catalyzed imine hydrogenation include: (a) Longley, C. J.; Goodwin, T.; Wilkinson, G. *Polyhedron* **1986**, *5*, 1625. (b) Becalski, A.; Cullen, W.; Fryzuk, M.; James, B. R.; Kang, G.; Rettig, S. *Inorg. Chem.* **1991**, *30*, 5002. (c) James, B. R.; Ball, G.; Cullen, W.; Fryzuk, M.; Henderson, W.; McFarlane, K. *Inorg. Chem.* **1994**, *33*, 1464. (d) Marcazzan, P.; Ezhova, M. B.; Patrick, B. O.; James, B. R. *C. R. Chim.* **2002**, *5*, 573. (e) Marcazzan, P.; Patrick, B. O.; James, B. R. *Inorg. Chem.* **2004**, *43*, 6838, and references therein.

(4) Examples of iridium-catalyzed imine hydrogenation include: (a) Cheong, Y.; Osborn, J. *J. Am. Chem. Soc.* **1990**, *112*, 9400. (b) Cheong, Y.; Meyer, D.; Osborn, J. *J. Chem. Soc., Chem. Commun.* **1990**, 869. (c) Osborn, J.; Sablong, R. *Tetrahedron Lett.* **1996**, *37*, 4937. (d) Guiu, E.; Muñoz, B.; Castillón, S.; Claver, C. *Adv. Synth. Catal.* **2003**, *345*, 169. (e) Dorta, R.; Broggini, D.; Kissner, R.; Togni, A. *Chem. Eur. J.* **2004**, *10*, 4546. (f) Miecznikowski, J. R.; Crabtree, R. H. *Polyhedron* **2004**, *23*, 2857, and references therein.

(5) Herrera, V.; Muñoz, B.; Landaeta, V.; Canudas, N. *J. Mol. Catal.* **2001**, *174*, 141.

(6) (a) Marcazzan, P.; Patrick, B. O.; James, B. R. *Organometallics* **2003**, *22*, 1177. (b) Marcazzan, P.; Abu-Gnim, C.; Seneviratne, K. N.; James, B. R. *Inorg. Chem.* **2004**, *43*, 4820. (c) Casey, C. P.; Johnson, J. B. *J. Am. Chem. Soc.* **2005**, *127*, 1883.

(7) Landaeta, V. R.; Peruzzini, M.; Herrera, V.; Bianchini, C.; Sánchez-Delgado, R. A.; Goeta, A.; Zanobini, F. *J. Organomet. Chem.*, in press.

10.1021/om0504912 CCC: $33.50
Publication on Web 12/09/2005

Scheme 2

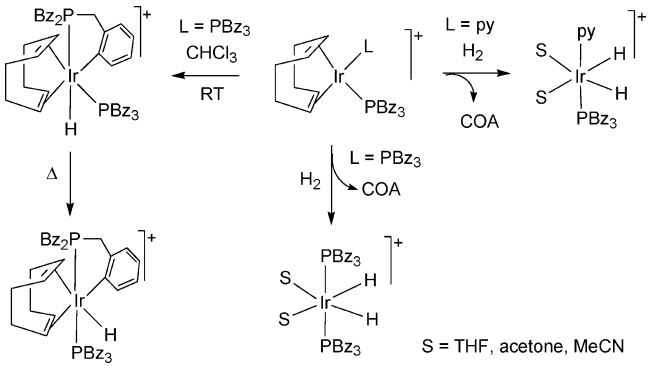

Scheme 3

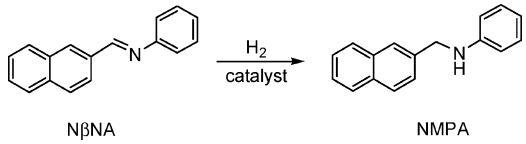

experiments, but they could not be isolated in the solid state due to fast decomposition.[7]

The reactivity of **1** and **2** towards H_2, together with the proven ability of the related Rh^I and Ir^I complexes $[M(PPh_3)_2(COD)]^+$ and $[M(py)(PPh_3)(COD)]^+$ (M = Rh, Ir; COD = 1,3-cyclooctadiene) to catalyze the hydrogenation of a variety of unsaturated substrates, including imines,[5,8,9] prompted us to explore the performance of the new PBz_3 complexes as catalysts for the reduction of *N*-(*β*-naphthylmethylene)aniline (N*β*NA) to naphthalene-2-ylmethylphenylamine (NMPA) (Scheme 3). Another motivation for carrying out the present study was that the use of PBz_3 in homogeneous catalysis was virtually unknown previous to this work, despite the fact that alkyl- and arylphosphines constitute the most extensively employed class of ligands in catalytic reactions. Indeed, the only reported example involving PBz_3 was the hydroformylation of allylbenzene by a rhodium catalyst generated in situ by mixing $[Rh(OAc)(COD)]_2$ and PBz_3.[10,11] Therefore, we felt that a study of the catalytic properties of metal-PBz_3 complexes would be of interest, as this tertiary phosphine lies amid PPh_3 and PCy_3 in terms of nucleophilic and steric properties.[12]

Table 1. Catalytic Hydrogenation of *N*-(*β*-Naphthylmethylene)aniline by PBz_3 Ir and Rh Complexes[a]

run	catalyst	conversion (%)
1	**1**	53
2	**2**	96
3	**4**	4
4	**5**	traces
5	**6**	1
6	**7**	3
7[b]	**3**	87

[a] Conditions: $p(H_2) = 13.8$ bar; $T = 25$ °C; 4 h; substrate:catalyst 100:1; THF = 5 mL. [b] 18 h, ref 5.

In this paper, we report a kinetic and mechanistic study of the hydrogenation of N*β*NA to NMPA catalyzed by the Ir^I complexes **1** and **2**. For comparative purposes, we have also examined the catalytic activity of $[Rh(PPh_3)_2(COD)]PF_6$ (**3**) and of various Rh and Ir complexes stabilized by PBz_3, namely, $IrCl(PBz_3)(COD)$ (**4**), $RhCl(PBz_3)(COD)$ (**5**), $[Rh(PBz_3)_2(COD)]PF_6$ (**6**), and $[Rh(py)(PBz_3)(COD)]PF_6$ (**7**).

Results and Discussion

Catalytic Hydrogenation of *N*-(*β*-Naphthylmethylene)aniline by Rhodium and Iridium Complexes. Batch hydrogenation reactions of N*β*NA were carried out in THF at room temperature under a H_2 pressure of 13.8 bar. The results obtained are collected in Table 1. All reactions were carried out at least once in the presence of an excess of elemental mercury, which is known to deactivate heterogeneous catalysis arising from the presence of metal particles or colloids in the mixtures.[13] In no case was a decrease in activity observed; besides this mercury test, the homogeneous nature of our reactions was also inferred by the excellent reproducibility of the kinetic measurements (see below), which is unlikely to be observed if the true catalyst is a decomposition product of the precursor.

Only the cationic iridium precursors **1** and **2** were able to generate efficient catalysts for N*β*NA hydrogenation under our reaction conditions (runs 1, 2). Neither the analogous rhodium complexes **6** and **7** (runs 5, 6) nor the neutral Ir or Rh complexes **4** and **5** (runs 3, 4) were able to hydrogenate the imine at a significant rate.

The much lower efficiency of rhodium catalysts as compared to iridium analogues in the hydrogenation of imine C=N bonds has been observed by several authors.[5,6] James and co-workers have recently demonstrated that rhodium-based catalysts may undergo deactivation by forming stable amine adducts.[6] However, this issue may not always be so simple, as other factors might play a role in controlling the catalytic activity of rhodium and iridium complexes. Indeed, if the strength of the $Rh-N_{amine}$ bond may account for the very low activity of the Rh complex **6** (run 5), it cannot explain why the PPh_3 rhodium complex **3** is a better catalyst[5] than the PBz_3 analogue **6** under identical reaction conditions [5 mol N*β*NA converted (mol **3** × h)$^{-1}$ vs 0.4 mol N*β*NA converted (mol **6** × h)$^{-1}$].

Aimed at gathering further information that might shed light on the factors controlling the activity of phosphine-modified rhodium and iridium catalysts, a kinetic study of the hydrogenation of N*β*NA catalyzed by **1**, **2**, and **3** (as a comparison standard) was undertaken, together with in situ NMR experiments. Also, structurally related PBz_3 and PPh_3 catalyst precur-

(8) (a) Crabtree, R. H.; Morris, G. E. *J. Organomet. Chem.* **1977**, *135*, 395. (b) Crabtree, R. H.; Gautier, A.; Giordano, G.; Khan, T. *J. Organomet. Chem.* **1977**, *141*, 113. (c) Crabtree, R. H. *Acc. Chem. Res.* **1979**, *12*, 331. (d) Haines, L. *Inorg. Nucl. Chem. Lett.* **1969**, *5*, 399. (e) Haines, L. *Inorg. Chem.* **1970**, *9*, 1517. (f) Haszeldine, R.; Lunt, R.; Parish, R. *J. Chem. Soc. A* **1971**, 3711. (g) Suggs, W. J.; Cox, S. D.; Crabtree, R. H.; Quirk, J. M. *Tetrahedron Lett.* **1981**, *22*, 203. (h) Crabtree, R. H. *Chem. Rev.* **1985**, *85*, 245.

(9) Crabtree, R. H.; Demou, P. C.; Eden, D.; Mihelcic, J. M.; Parnell, C. A.; Quirk, J. M.; Morris, G. E. *J. Am. Chem. Soc.* **1982**, *104*, 6994.

(10) da Silva, A. C.; de Oliveira, K. C. B.; Gusevskaya, E. V.; dos Santos, E. N. *J. Mol. Catal.* **2002**, *179*, 133.

(11) Barros, H. J. V.; Ospina, M. L.; Arguello, E.; Rocha, W. R.; Gusevskaya, E. V.; dos Santos, E. N. *J. Organomet. Chem.* **2003**, *671*, 150.

(12) The cone angle of PBz_3 is about 165°, i.e., much larger than that of PPh_3 (145°), but similar to that of PCy_3 (170°). For some references on the basicity and steric hindrance of these and other phosphine ligands, see: (a) Streuli, C. A. *Anal. Chem.* **1960**, *32*, 985. (b) Tolman, C. *J. Am. Chem. Soc.* **1970**, *92*, 2953. (c) Tolman, C. *J. Am. Chem. Soc.* **1970**, *92*, 2956. (d) Tolman, C.; Seidel, W.; Gosser, W. *J. Am. Chem. Soc.* **1974**, *96*, 53. (e) Tolman, C. *Chem. Rev.* **1977**, *77*, 313. (f) Allman, T.; Goel, R. G. *Can. J. Chem.* **1982**, *60*, 716. (g) Wilkes, L. M.; Nelson, J. H.; Mitchener, J. P.; Babich, M. W.; Riley, W. C.; Helland, B. J.; Jacobson, R. A.; Yu Cheng, M.; Seff, K.; McCusker, L. *Inorg. Chem.* **1982**, *21*, 1376. (h) Johansson, M. H.; Otto, S.; Oskarsson, Å. *Acta Crystallogr. B* **2002**, *58*, 244. (i) Muller, A.; Roodt, A.; Otto S.; Oskarsson, Å.; Yong, S. *Acta Crystallogr. E* **2002**, *58*, m715.

(13) (a) Crabtree, R.; Anton, D. R. *Organometallics* **1983**, *2*, 855. (b) Whitesides, G. S.; Racket, M.; Brainard, R. L.; Lavalleye, J. P.; Sowinski, A. F.; Izumi, A. N.; Moore, S. S.; Brawn, D. W.; Staudt, E. M. *Organometallics* **1985**, *4*, 1819.

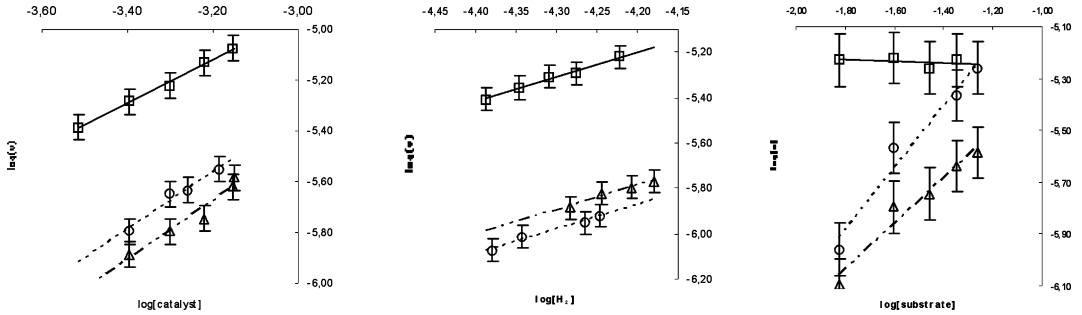

[Ir(COD)(PBz$_3$)$_2$]PF$_6$ (**1**) ○ [Ir(COD)(py)(PBz$_3$)]PF$_6$ (**2**) △ [Rh(COD)(PPh$_3$)$_2$]PF$_6$ (**3**)

Figure 1. Effect of catalyst, imine, and hydrogen concentrations on the rate of hydrogenation of NβNA catalyzed by **1**, **2**, and **3**.

sors were investigated in an attempt to establish phosphine structure−activity relationships.

Kinetic Studies. The kinetics of the hydrogenation of NβNA by **1**, **2**, and **3** were studied in THF in the temperature range from 304 to 336 K at subatmospheric pressure with H_2 initial concentrations varying from 4.1×10^{-5} to 6×10^{-5} M. The reactions were carried out at different catalyst, substrate, and hydrogen concentrations, and the corresponding kinetic data are reported in the Supporting Information (Tables S1−S3).

Irrespective of the catalyst precursor, the initial rates (v_i) showed a linear dependence on catalyst concentration, as evidenced by plots of log v_i against log[cat], which yielded straight lines with slopes of 0.99 for **1**, 1.1 for **2**, and 1.1 for **3** (Figure 1a). No appreciable effect of substrate concentration was observed for **1** (Figure 1c). A zero-order rate in substrate concentration has been reported for other imine hydrogenation reactions.[6b] On the other hand, a first-order dependence with respect to substrate concentration was found for both **2** and **3** (the slope values of the plots log v_i vs log[NβNA] were 1.10 and 0.99, respectively). Finally, for all metal precursors, a first-order dependence on hydrogen concentration was shown by the plots log v_i vs log[H_2] (Figure 1b) with slope values of 1.0 (eq 1), 1.1 (eq 2), and 1.1 (eq 3).

Incorporation of all these data provided the experimental rate laws indicated by eqs 1−3 for **1**, **2**, and **3**, respectively:

$$v_i = \mathrm{d[amine]}/\mathrm{d}t = k_{cat}[\mathrm{Ir}][\mathrm{H_2}] \quad (1)$$

$$v_i = \mathrm{d[amine]}/\mathrm{d}t = k_{cat}[\mathrm{Ir}][\mathrm{N}\beta\mathrm{NA}][\mathrm{H_2}] \quad (2)$$

$$v_i = \mathrm{d[amine]}/\mathrm{d}t = k_{cat}[\mathrm{Rh}][\mathrm{N}\beta\mathrm{NA}][\mathrm{H_2}] \quad (3)$$

The average values of the observed catalytic rate constants for **1** and **2** at 318 K and for **3** at 329 K, calculated from eqs 1, 2, and 3, respectively, using the data in Tables S1−S3, are $k_{cat(Ir\ 1)} = (18.6 \pm 0.1) \times 10^3\ M^{-1}\ s^{-1}$, $k_{cat(Ir\ 2)} = (3.1 \pm 0.2) \times 10^3\ M^{-2}\ s^{-1}$, and $k_{cat(Rh\ 3)} = (2.1 \pm 0.1) \times 10^3\ M^{-2}\ s^{-1}$.

In summary, the hydrogenation reaction assisted by the Ir precursor **1** follows a second-order law (eq 1), whereas both the Ir complex **2** (eq 2) and the Rh complex **3** (eq 3) exhibit a third-order rate law, analogous to the one previously reported by some of us for NβNA hydrogenation catalyzed by [Ir(PPh$_3$)$_2$(COD)]PF$_6$ in THF ($k_{cat} = (2.2 \pm 0.3) \times 10^3\ M^{-2}\ s^{-1}$ at 323 K).[5] From a comparison of the k_{cat} values, the catalytic activity of these complexes follows the order **1** > **2** > **3** ≈ [Ir(PPh$_3$)$_2$(COD)]PF$_6$.

Proposed Mechanism for the Hydrogenation of NβNA Catalyzed by [Ir(PBz$_3$)$_2$(COD)]PF$_6$ (1). As shown in Scheme 1, complex **1** undergoes a spontaneous intramolecular *o*-metalation in solution and reacts with H_2 in either acetone or THF to give *cis*-bis(solvento) dihydrides [Ir(H)$_2$(S)$_2$(PBz$_3$)$_2$]PF$_6$ [S = acetone (**8**), THF (**9**)] and free cyclooctane (COA).[7] The latter complex is also formed by reaction of the *o*-metalated complex with H_2.

When a THF-d_8 solution of **9** was treated with 2 equiv of NβNA, NMR spectroscopy showed that the hydride triplet in the parent compound (δ −23.5, J_{HP} = 15.5 Hz) was rapidly replaced by another triplet at −18.42 ppm with an identical coupling constant to phosphorus (J_{HP} = 15.5 Hz), while free THF was produced. This evidence, together with the appearance of a new singlet in the $^{31}P\{^1H\}$ NMR spectrum at 12.0 ppm (the $^{31}P\{^1H\}$NMR spectrum of **9** consists of a singlet at 9.83 ppm),[7] is strongly indicative of the formation of the *cis*-bis(imine) complex [Ir(H)$_2$(NβNA)$_2$(PBz$_3$)$_2$]PF$_6$ (**10**), which unfortunately could not be isolated, as it was unstable with respect to intramolecular hydrogen transfer from iridium to a coordinated NβNA molecule to presumably yield [Ir(NβNA)(NMPA)(PBz$_3$)$_2$]PF$_6$ (**11**) (eq 4).

$$[\mathrm{Ir(H)_2(N}\beta\mathrm{NA)_2(PBz_3)_2}]\mathrm{PF_6} \rightleftharpoons [\mathrm{Ir(N}\beta\mathrm{NA)(NMPA)(PBz_3)_2}]\mathrm{PF_6} \quad (4)$$

Therefore, **10** may be considered as an active species in the catalytic hydrogenation of NβNA by **1**, and we suggest that the subsequent reaction of the reduced intermediate **11** with H_2 depicted in eq 5 is the rate-determining step (k_2) of the catalytic cycle, leading to the dihydride [IrH$_2$(NβNA)(NMPA)(PBz$_3$)$_2$]PF$_6$ (**12**).

$$[\mathrm{Ir(N}\beta\mathrm{NA)(NMPA)(PBz_3)_2}]\mathrm{PF_6} + \mathrm{H_2} \xrightarrow{k_2} [\mathrm{IrH_2(N}\beta\mathrm{NA)(NMPA)(PBz_3)_2}]\mathrm{PF_6} \quad (5)$$

Fast replacement of the product amine by an imine in **12** would complete the cycle and regenerate **10** (eq 6).

$$[\mathrm{IrH_2(N}\beta\mathrm{NA)(NMPA)(PBz_3)_2}]\mathrm{PF_6} + \mathrm{N}\beta\mathrm{NA} \xrightarrow{K_3} [\mathrm{IrH_2(N}\beta\mathrm{NA)_2(PBz_3)_2}]\mathrm{PF_6} + \mathrm{NMPA} \quad (6)$$

A rate law accounting for this mechanism can be derived from eq 7:

$$v_i = \mathrm{d[amine]}/\mathrm{d}t = \boldsymbol{k_2}[\mathbf{11}] \quad (7)$$

Considering the equilibrium in eq 4 and the mass balance for iridium ([Ir]$_0$ = [**10**] + [**11**]), the concentration of **11** may be expressed as in eq 8:

$$[\mathbf{11}] = K_1[\mathrm{Ir}]_0/(1 + K_1) \quad (8)$$

and substituting [**11**] in eq 7, we arrive at the rate law shown in eq 9:

$$v_i = k_2K_1[\mathrm{Ir}]_0[\mathrm{H_2}]/(1 + K_1) \quad (9)$$

In agreement with the fact that the only species observed by NMR was complex **10**, we can assume that under our reaction conditions $K_1 \ll 1$; eq 8 is then approximated to [**11**] = $K_1[\mathrm{Ir}]_0$, and the rate expression can be simplified as in eq 10, which is identical to the experimental rate law if $k_{cat} = k_2K_1$.

$$v_i = k_2K_1[\mathrm{Ir}]_0[\mathrm{H_2}] \quad (10)$$

The combined kinetic and NMR experiments allow us to propose a catalytic cycle for the hydrogenation of NβNA by **1** where the precursor is rapidly hydrogenated to form an octahedral dihydrido-bis-imine intermediate, which reversibly undergoes intramolecular hydride transfer to give a coordinated amine (Scheme 4). This intermediate then oxidatively adds dihydrogen as the rate-determining step to yield a dihydrido species containing both coordinated imine and amine. Displacement of the product by a new incoming imine molecule regenerates the active species and completes the cycle. Noteworthy, a rhodium amine-imine intermediate species has been detected by James and co-workers along the homogeneous hydrogenation of $PhCH_2N{=}CHPh$ by $[Rh(PPh_3)_2(COD)]PF_6$.[3e,6b]

Proposed Mechanism for the Hydrogenation of NβNA by [Ir(py)(PBz$_3$)(COD)]PF$_6$ (2). Like **1**, the py derivative **2** reacts readily with H_2 in THF-d_8 to yield the *cis*-bis(solvento) dihydride $[Ir(H)_2(THF)_2(py)(PBz_3)]PF_6$ (**13**). This complex was prepared and identified by in situ NMR experiments in THF-d_8 (hydride doublet at −19.8 ppm with a *cis*-HP coupling of 16.8 Hz).[7] When NβNA (2 equiv) was added to a solution of **13**, fast displacement of the solvent molecules occurred with formation of two new major species featured by $^{31}P\{^1H\}$ NMR singlets at 7.2 and 6.5 ppm and ^1H NMR hydride signals at 16.5 (J_{HP} = 15.4 Hz) and 16.2 ppm (J_{HP} = 15.5 Hz), respectively. Since the addition of a further 2 equiv of NβNA increased the concentration of the product with the ^{31}P NMR singlet at 6.5 ppm at the expense of the other one, the complex with the 7.2 ppm signal is most likely the mono-imine intermediate $[Ir(H)_2(N\beta NA)(THF\text{-}d_8)(py)(PBz_3)]PF_6$ (**14**), which transforms into the bis-imine adduct $[Ir(H)_2(N\beta NA)_2(py)(PBz_3)]PF_6$ (**15**) in the presence of excess imine.

From a mechanistic viewpoint, the catalytic hydrogenation of the imine would therefore involve the preliminary reaction of the COD precursor **2** with H_2 and solvent molecules (THF) to give **13** and free COA, which is a peripheral reaction outside the catalytic cycle, followed by coordination of *one* imine molecule to form **14** via the reaction shown in eq 11. Coordination of a second imine molecule through the equilibrium K_1 (eq 12) leads to the formation of the bis(imine) intermediate **15**, as in eq 12.

$$[Ir(H)_2(THF)_2(py)(PBz_3)]^+ + N\beta NA \rightarrow [Ir(H)_2(N\beta NA)(THF)(py)(PBz_3)]^+ \quad (11)$$

$$[Ir(H)_2(N\beta NA)(THF)(py)(PBz_3)]^+ + N\beta NA \overset{K_1}{\rightleftharpoons} [Ir(H)_2(N\beta NA)_2(py)(PBz_3)]^+ \quad (12)$$

Scheme 4

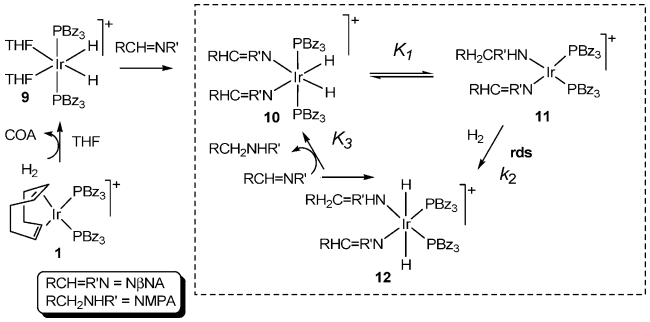

Reversible hydride transfer in **15** as shown in eq 13 (K_2) would yield a new species, $[Ir(N\beta NA)(NMPA)(py)(PBz_3)]^+$ (**16**), containing the hydrogenated product NMPA. The rate-determining addition of hydrogen to **16** (k_3) completes the cycle by releasing the product with concomitant formation of complex **14** (eq 13).

$$[Ir(H)_2(N\beta NA)_2(py)(PBz_3)]^+ \overset{K_2}{\rightleftharpoons} [Ir(N\beta NA)(NMPA)(py)(PBz_3)]^+ \quad (13)$$

$$[Ir(N\beta NA)(NMPA)(py)(PBz_3)]^+ + H_2 \xrightarrow{k_3} [Ir(H)_2(N\beta NA)(THF)(py)(PBz_3)]^+ + NMPA \quad (14)$$

According to this mechanistic picture, a rate law can be derived, taking into account that the initial rate of product formation is represented by eq 15:

$$v_i = d[\text{amine}]/dt = k_3[\mathbf{16}][\mathrm{H_2}] \quad (15)$$

Considering the equilibria in eqs 12 and 13 and the mass balance for iridium ($[Ir]_0$ = [**14**] + [**15**] + [**16**]) the concentration of **16** can be expressed as in eq 16:

$$[\mathbf{16}] = K_1K_2[\mathrm{Ir}]_0[N\beta NA]/(1 + K_1[N\beta NA] + K_1K_2[N\beta NA]) \quad (16)$$

which can be substituted in eq 15 to obtain:

$$v_i = K_1K_2k_3[\mathrm{Ir}]_0[N\beta NA][\mathrm{H_2}]/(1 + K_1[N\beta NA] + K_1K_2[N\beta NA]) \quad (17)$$

If the term $K_1[N\beta NA] + K_1K_2[N\beta NA] \ll 1$, the rate expression can be approximated to eq 18, which is identical to the experimental rate law provided that $k_{cat} = K_1K_2k_3$:

$$v_i = K_1K_2k_3[\mathrm{Ir}]_0[N\beta NA][\mathrm{H_2}] \quad (18)$$

This is a reasonable assumption, since it implies that the major species in solution is **14**, in agreement with our spectroscopic observations. Incorporation of the kinetic and NMR experiments leads to the catalytic cycle shown in Scheme 5 for the hydrogenation of NβNA by **2**.

Proposed Mechanism for the Hydrogenation of NβNA Catalyzed by [Rh(COD)(PPh$_3$)$_2$]PF$_6$ (3). To complement the experimental kinetic study of the hydrogenation of NβNA catalyzed by the Rh precursor **3**, we have carried out an in situ NMR study of the reactions of the latter complex with imine and H_2 in THF-d_8. It has been previously reported by Osborn[14]

(14) (a) Shapley, J. R.; Schrock, R. R.; Osborn, J. A. *J. Am. Chem. Soc.* **1969**, *91*, 2816. (b) Schrock, R. R.; Osborn, J. A. *J. Am. Chem. Soc.* **1976**, *98*, 2134.

Scheme 5

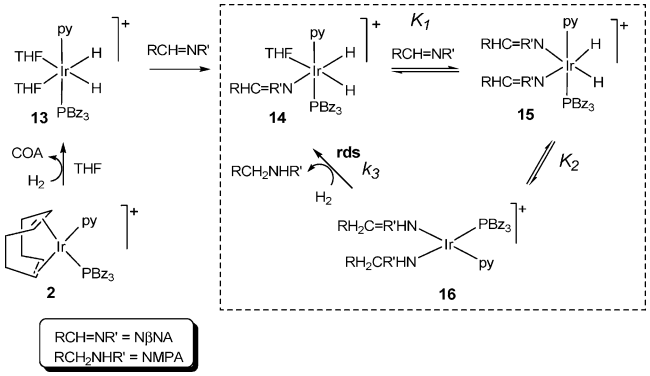

and other authors[8,9,13] that **3** reacts with hydrogen in coordinating solvents to give bis-solvento dihydrides with the formula $[Rh(H)_2(S)_2(PPh_3)_2]PF_6$ (S = solvent). Compound $[Rh(H)_2(THF\text{-}d_8)_2(PPh_3)_2]PF_6$ (**17**) was then generated in situ by bubbling H_2 into a THF-d_8 solution of **3**. The reaction of **17** at room temperature with 1 equiv of NβNA afforded a new species with cis dihydride ligands and trans P atoms (^{1}H NMR spectrum featured by a pseudoquartet at −16.2 ppm with $J_{HP} \cong J_{HRh} =$ 15.0 Hz and $^{31}P\{^1H\}$ NMR spectrum consisting of a doublet at 38.5 ppm, $J_{RhP} = 135.5$ Hz). The addition of a second equivalent of imine did not change the spectrum, except for slightly broadening the NMR signals. We suggest that the first product is the dihydride imine complex $[Rh(H)_2(N\beta NA)(THF\text{-}d_8)(PPh_3)_2]PF_6$ (**18**), which undergoes fast exchange of THF-d_8 between the two sites trans to P.[3b,6b] Complex **18** seems to remain the largely prevailing species even in the presence of a second equivalent of imine, although it is likely that an equilibrium with the bis-imine complex $[Rh(H)_2(N\beta NA)_2(PPh_3)_2]PF_6$ (**19**) may ensue. The latter complex would be in very low concentration, yet kinetically important. Indeed, all our attempts to isolate either **18** or **19** were unsuccessful, as only a Rh^I complex with no hydride ligands was obtained. The ^{1}H NMR spectrum of this new species contained a singlet at δ 9.84, attributable to the coordinated imine hydrogens C*H*═N, while the $^{31}P\{^1H\}$ NMR spectrum showed a doublet at 53.4 ppm ($J_{PRh} = 152$ Hz). It is therefore likely that, upon reductive elimination of H_2, a square-planar Rh^I complex, $[Rh(N\beta NA)_2(PPh_3)_2]PF_6$ (**20**), is formed. Facile elimination of H_2 is not an unexpected process for Rh^{III} dihydrides,[15] including PBz_3 complexes such as $[Rh(H)_2(Me_2CO\text{-}d_6)_2(PBz_3)_2]^+$ and $[Rh(H)_2(THF\text{-}d_8)_2(PBz_3)_2]^+$.[7] Whether the imines are η^1-*N* or η^2-*C*,*N* coordinated is difficult to assess on the exclusive basis of the NMR parameters. However, we are inclined to suggest an η^1-*N* mode in view of the X-ray structure of *cis*-$\{Rh[P(p\text{-tolyl})_3]_2(PhCH_2N{=}CHPh)(NH_2CH_2Ph)\}PF_6$ reported by James, where $PhCH_2N{=}CHPh$ acts as a monodentate ligand.[6b] Moreover, James and co-workers have proposed the formation of a similar η^1-*N* square-planar intermediate along the hydrogenation of *N*-(benzylidene)aniline catalyzed by $[Rh(H)_2(MeOH)_2(PPh_3)_2]PF_6$.[3b,e]

On the basis of the data presented above, we propose that, under catalytic conditions, **3** reacts in THF with hydrogen to give **17**, which may coordinate one or two NβNA molecules to form **18** in equilibrium with **19** (eq 19).

$$[Rh(H)_2(N\beta NA)(THF)(PPh_3)_2]PF_6 + N\beta NA \overset{K_1}{\rightleftharpoons} [Rh(H)_2(N\beta NA)_2(PPh_3)_2]PF_6 + THF \quad (19)$$

Since the rate law for catalyst **3** is similar to that of catalyst **2**, it is reasonable to assume that the mechanisms are also similar, and therefore the kinetic data may be treated in an analogous way. Hydrogen transfer to NβNA in complex **19** gives the Rh^I complex $[Rh(N\beta NA)(NMPA)(PPh_3)_2]PF_6$ (**21**) containing the hydrogenated product NMPA (eq 20), and the catalytic cycle is completed by oxidatively adding H_2 as the rate-determining step, to release the product and regenerate **18** (eq 21).

$$[Rh(H)_2(N\beta NA)_2(PPh_3)_2]PF_6 \overset{K_2}{\rightleftharpoons} [Rh(N\beta NA)(NMPA)(PPh_3)_2]PF_6 \quad (20)$$

$$[Rh(N\beta NA)(NMPA)(PPh_3)_2]PF_6 + H_2 \xrightarrow{k_3} [Rh(H)_2(N\beta NA)(THF)(PPh_3)_2]PF_6 + NMPA \quad (21)$$

As for the case of **2**, a rate law can be derived, taking into account the initial rate of product formation shown in eq 22:

$$v_i = d[amine]/dt = k_3[\mathbf{21}][H_2] \quad (22)$$

Considering the equilibria reported in eqs 19 and 20 and the mass balance for rhodium ($[Rh]_0 = [\mathbf{18}] + [\mathbf{19}] + [\mathbf{21}]$), the concentration of **21** can be expressed as in eq 23:

$$[\mathbf{21}] = K_1K_2[Rh]_0[N\beta NA]/(1 + K_1[N\beta NA] + K_1K_2[N\beta NA]) \quad (23)$$

which leads to

$$v_i = K_1K_2k_3[Rh]_0[N\beta NA][H_2]/(1 + K_1[N\beta NA] + K_1K_2[N\beta NA]) \quad (24)$$

If we then assume the term $K_1[N\beta NA] + K_1K_2[N\beta NA] \ll 1$ as before, the rate expression can be approximated to

$$v_i = K_1K_2k_3[Rh]_0[N\beta NA][H_2] \quad (25)$$

which is identical to the experimental rate law when $k_{cat} = K_1K_2k_3$.

A mechanism for the hydrogenation of NβNA catalyzed by **3**, which incorporates the results of the NMR and kinetic study, is shown in Scheme 6. Within this mechanistic picture, **18** is the major species, as observed by NMR, and both **17** and **20** lie outside of the catalytic cycle.

Activation Parameters of the Hydrogenation of NβNA by 1, 2, and 3. The effect of temperature on the rate constants in the hydrogenation of NβNA by **1**, **2**, and **3** was studied in the range from 307 to 336 K, from 302 to 323 K, and from 304 to 323 K, respectively, under the following experimental conditions: $[N\beta NA] = 2.5 \times 10^{-2}$ M, [catalyst] = $5.0 \times 1\ 0^{-4}$ M, and $[H_2] = 6.0 \times 10^{-5}$ M. Within these ranges, the variation of the H_2 solubility with the temperature was negligible in THF.[16] Plotting ln k_{cat} vs $1/T$ (Figure 2) allowed us to evaluate the activation energy E_a, the frequency factor *A*, the extrapolated value of the rate constant at 298 K, and the values of enthalpy, entropy, and free energy of activation. The resulting data are listed in Table 2.

(15) See for example: Bianchini, C.; Masi, D.; Meli, A.; Peruzzini, M.; Zanobini, F. *J. Am. Chem. Soc.* **1988**, *110*, 6411.

(16) For H_2 solubility at different temperatures in common organic solvents see: (a) Waters, J.; Mortimer, G.; Clements, H. *J. Chem. Eng. Data* **1970**, *15*, 174. (b) Brunner, E. *Ber. Bunsen-Ges. Phys. Chem.* **1979**, *83*, 715. (c) Brunner, E. *J. Chem. Eng. Data* **1985**, *30*, 269. (d) International Union of Pure and Applied Chemistry, IUPAC. *Solubility Data Series: Hydrogen and Deuterium*, *5/6*, 219.

Scheme 6

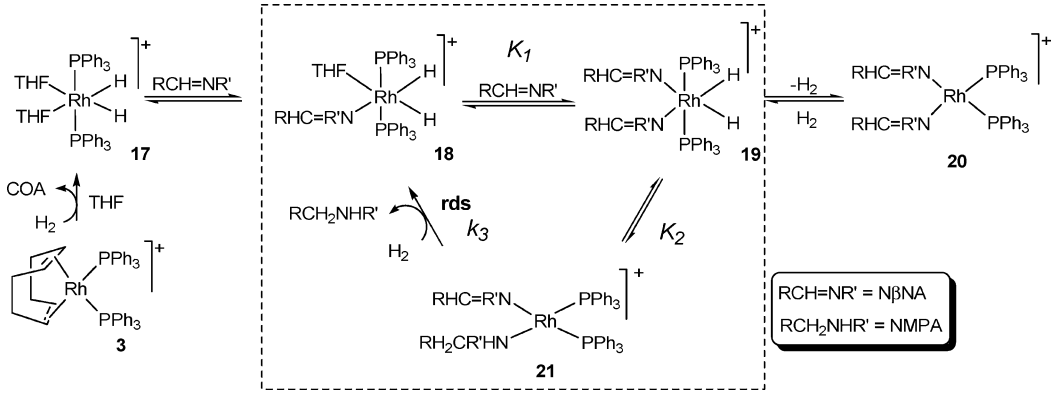

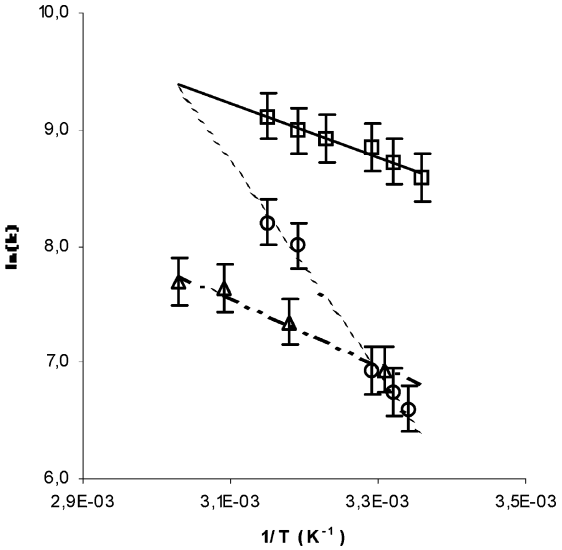

Figure 2. Effect of reaction temperature on the hydrogenation of NβNA catalyzed by **1**, **2**, and **3**.

Table 2. Activation Parameters for the Hydrogenation of NβNA Using 1, 2, and 3 as Catalyst Precursors

	1	**2**	**3**
E_a (kcal/mol)	4.6 ± 0.2	15.8 ± 0.2	5.4 ± 0.3
A	$(1.2 \pm 0.2) \times 10^7$ $M^{-1}\,s^{-1}$	$(1.6 \pm 0.4) \times 10^{14}$ $M^{-2}\,s^{-1}$	$(7.3 \pm 0.4) \times 10^6$ $M^{-2}\,s^{-1}$
k_{cat}(25 °C)	5007.0 $M^{-1}\,s^{-1}$	389.2 $M^{-2}\,s^{-1}$	845.2 $M^{-2}\,s^{-1}$
$\Delta H^{\ddagger}$ (kcal/mol)	4.0 ± 0.2	15.2 ± 0.3	4.8 ± 0.3
$\Delta S^{\ddagger}$ (eu)	−53 ± 1	−52 ± 3	−55 ± 2
$\Delta G^{\ddagger}$ (kcal/mol)	20 ± 1	31 ± 2	21 ± 2

A negative value for $\Delta S^{\ddagger}$ has been found for all complexes, as is expected for associative transition states. The positive $\Delta G^{\ddagger}$ and $\Delta H^{\ddagger}$ values are comparable to those reported for the hydrogenation of unsaturated molecules with C═X bonds (X = heteroatom) by analogous rhodium and iridium catalysts.[5,17] Provided the value of k_{cat} at 298 K is taken as a measure of the catalytic activity, the most efficient catalytic system is generated by the bis-PBz_3 precursor **1**, while the PPh_3-modified precursor **3** is twice as active as the py adduct **2**.

Conclusions

A family of Rh and Ir complexes stabilized by PBz_3 ligands have been tested as catalyst precursors for the hydrogenation of NβNA to NMPA, and their catalytic efficiency has been compared with that of the structurally related PPh_3 rhodium and iridium catalysts $[M(PPh_3)_2(COD)]PF_6$.[5] Under comparable experimental conditions, the PBz_3-modified catalysts are by far more efficient than the PPh_3-modified analogues. In particular, the batch catalytic reactions have shown that the turnover frequency [mol NMPA produced (mol cat × h)$^{-1}$] decreases in the order $[Ir(py)(PBz_3)_2(COD)]^+$ (24) > $[Ir(PBz_3)_2(COD)]^+$ (13) > $[Ir(PPh_3)_2(COD)]^+ = [Rh(PPh_3)_2(COD)]^+$ (5).[5] This finding is interesting and may stimulate further studies of the catalytic activity of PBz_3 metal complexes in homogeneous processes. The better performance of **2** vs **1** in batch conditions (Table 1 and ref 5) may be due to significant incorporation of iridium sites of **1** into inactive *o*-metalated species (Scheme 2), while the formation of stronger bonds to the amine product may well account for the lower activity of the Rh precursor **3** (Schemes 5 and 6).[3e]

Except for the position of the py precursor **2**, the order of activity found in the batch reactions agrees with the results of the kinetic study as the k_{cat}(298 K) values have been found to decrease in the order $[Ir(PBz_3)_2(COD)]^+$ (5007 $M^{-1}\,s^{-1}$) > $[Rh(PPh_3)_2(COD)]^+$ (845.2 $M^{-2}\,s^{-1}$) > $[Ir(py)(PBz_3)_2(COD)]^+$ (389.2 $M^{-2}\,s^{-1}$).

Discrepancies between tof and v_i are frequently encountered in homogeneous catalysis. In the present case, the discrepancy may be due to the large pressure difference. It may also be possible that at the higher pressure of the batch reactions the kinetic laws are different from those at low pressure and hence the reaction order may change.

Experimental Section

General Information. All reactions and manipulations were routinely performed under a dry nitrogen or argon atmosphere using standard Schlenk techniques. ^1H and $^{13}C\{^1H\}$ spectra were recorded on either a Bruker ACP 200 (200.13 and 50.32 MHz) or a Bruker AM 300 (300.13 and 75.47 MHz) spectrometer. Peak positions are relative to tetramethylsilane and were calibrated against the residual solvent resonance (^1H) or the deuterated solvent multiplet (^{13}C). $^{31}P\{^1H\}$ NMR spectra were recorded on the same instruments operating at 81.01 and 121.49 MHz, respectively. Chemical shifts were measured relative to external 85% H_3PO_4, with downfield shifts considered positive. All the NMR spectra were recorded at room temperature (25 °C) unless otherwise stated. GC analyses were performed on a HP-5890 equipped with a mass selective detector HP-5972 (GC-MS) and a DB-5 capillary column. Reactions under controlled gas pressure were performed on Parr reactors.

Materials. Unless otherwise stated, all solvents were distilled just prior to use from appropriate drying agents. Dichloromethane, methanol, and THF were distilled from $CaSO_4$, P_2O_5, and sodium/

(17) Sánchez-Delgado, R.; Rosales, M. *Coord. Chem. Rev.* **2000**, *196*, 249.

(18) Taguchi, K.; Westheimer, F. *J. Org. Chem.* **1971**, *36*, 1570.

benzophenone, respectively. Diethyl ether and petroleum ether were dried with sodium. Aniline (Aldrich) was purified by reduced pressure distillation. Hydrogen was purified by passing it through two columns in series containing CuO/Al_2O_3 and $CaSO_4$, respectively. Deuterated solvents were dried over 4 Å molecular sieves prior to use. All other chemicals were commercial products and used as received without further purification. Literature methods were employed for the synthesis of $MCl(PBz_3)_2(COD)$ (M = Rh, Ir),[7] $[M(PBz_3)_2(COD)]PF_6$ (M = Rh, Ir),[7] $[M(py)(PBz_3)(COD)]PF_6$ (M = Rh, Ir),[7] $[Rh(PPh_3)_2(COD)]PF_6$,[14] and *N*-(*β*-naphthylmethylene)aniline.[18] The solid complexes were collected on a sintered glass frit and washed with ethanol and light petroleum ether (bp 40−60 °C) or pentane before being dried in a stream of nitrogen.

Catalytic Experiments. In a typical experiment a solution of the catalyst precursor and a 100-fold excess of N*β*NA in THF was placed into a Parr reactor (15 mL). After loading of the reactants of the catalytic system, the reactor was flushed with H_2 to remove oxygen and then pressurized to the desired pressure at room temperature, heated to the proper temperature, and immediately stirred. After the desired time, the reactor was cooled to room temperature and slowly depressurized. A sample of the solution was withdrawn and analyzed by GC-MS. Each run was repeated at least twice to ensure reproducibility of the results.

Kinetic Measurements. In a typical experiment, a solution of the catalyst and N*β*NA (substrate:catalyst = 50:1) in THF (50 mL) was placed in a glass reactor fitted with a reflux condenser kept at 10 °C. The reactor was sealed with Apiezon wax to a high-vacuum line, and the solution was carefully degassed by three freeze−pump−thaw cycles; hydrogen was admitted at this point to the desired pressure, an electric oven preheated to the required temperature was placed around the reactor, and magnetic stirring was immediately begun. The reaction was followed by measuring the drop of the hydrogen pressure as a function of time. Each run was repeated at least twice to ensure reproducibility of the results. To use the initial rate method, the conversion of reactants in the catalytic reactions was generally (although not necessarily) kept below 10% (ca. 5−20 turnovers). The measured $\Delta P(H_2)$ values were converted to mmol of amine product, and the data were plotted as molar concentration of the product as a function of time, yielding straight lines; the initial hydrogenation rates were obtained from the corresponding slopes. All straight lines were fitted by conventional linear regression programs to $r^2 > 0.97$. The hydrogen concentration in solution under the reaction conditions was calculated according to published solubility data.[16]

In Situ NMR Experiments. Reaction of $[Ir(H)_2(THF)_2(PBz_3)_2]PF_6$ (9) with N*β*NA. Complex **1** (0.03 mmol) was dissolved in 1 mL of THF-d_8 directly in a 5 mm NMR tube. H_2 was gently bubbled into the solution with a long syringe needle at 0 °C for the time, indicated by previous NMR experiments, required to convert all **1** into the dihydride **9**. After bubbling N_2 into the tube for 2 min at −10 °C, 2 equiv of N*β*NA were added into the tube. ^1H and $^{31}P\{^1H\}$ NMR spectra, immediately acquired at −10 °C, showed the selective formation of $[Ir(H)_2(N\beta NA)_2(PBz_3)_2]PF_6$ (**10**). ^1H NMR (THF-d_8, 300.13 MHz): δ −18.42 (t, hydrides, J_{HP} = 15.5 Hz). $^{31}P\{^1H\}$ NMR (THF-d_8, 121.49 MHz): δ 12.0 ppm (s).

Reaction of $[Ir(H)_2(THF\text{-}d_8)_2(py)(PBz_3)]PF_6$ (13) with N*β*NA. Complex **2** (0.03 mmol) was dissolved in 1 mL of THF-d_8 directly in a 5 mm NMR tube. H_2 was gently bubbled into the solution with a long syringe needle at 0 °C for the time, indicated by previous NMR experiments, required to convert all **2** into the dihydride **13**. After bubbling N_2 into the tube for 2 min at −10 °C, 2 equiv of N*β*NA were added into the tube. ^1H and $^{31}P\{^1H\}$ NMR spectra, immediately acquired at −10 °C, showed the formation of two major Rh complexes in a ca. 2:1 ratio, along with other compounds in very low concentration. Addition of further N*β*NA (2 equiv) changed the product ratio to 1:3. The product that forms in larger concentration after addition of 2 equiv of N*β*NA is assigned the formula $[Ir(H)_2(N\beta NA)(THF\text{-}d_8)(py)(PBz_3)]PF_6$ (**14**). The other product is assigned the bis-imine structure $[Ir(H)_2(N\beta NA)_2(py)(PBz_3)]PF_6$ (**15**).

Selected NMR data for **14**: $^{31}P\{^1H\}$ NMR (THF-d_8, 121.49 MHz): δ 7.2 (s). ^1H NMR (THF-d_8, 300.13 MHz): δ −16.5 (d, Ir−H, J_{HP} = 15.4 Hz). The observation of a single ^1H NMR resonance for the two nonequivalent hydrides is likely due to fast exchange of coordinated and free THF, which averages the spectrum.

Selected NMR data for **15**: $^{31}P\{^1H\}$ NMR (THF-d_8, 121.49 MHz): δ 6.5 (s). ^1H NMR (THF-d_8, 300.13 MHz): δ −16.2 (d, Ir−H, J_{HP} = 15.5 Hz).

Reaction of $[Rh(H)_2(THF\text{-}d_8)_2(PPh_3)_2]PF_6$ (17) with N*β*NA. Complex **3** (0.03 mmol) was dissolved in 1 mL of THF-d_8 directly in a 5 mm NMR tube. H_2 was gently bubbled into the solution with a long syringe needle at 0 °C for the time, indicated by previous NMR experiments, required to convert all **3** into the dihydride **17**. After bubbling N_2 into the tube for 2 min at −10 °C, 1 equiv of N*β*NA was added into the tube. A ^1H NMR spectrum was immediately acquired at −10 °C, showing the formation of a species featured by a pseudoquartet at δ −16.2 ($J_{HP} \cong J_{HRh}$ = 15.0 Hz). The $^{31}P\{^1H\}$ NMR spectrum consisted of a doublet at 38.5 ppm (J_{PRh} = 135.5 Hz). The addition of a second equivalent of imine did not change appreciably the NMR spectra, except for a slight broadening of the ^{31}P signals. Heating the NMR probe to 20 °C under nitrogen led to the disappearance of this complex with formation of a new compound that we suggest to be $[Rh(N\beta NA)_2(PPh_3)_2]PF_6$ (**20**) on the basis of the $^{31}P\{^1H\}$ NMR (THF-d_8, 121.49 MHz), showing a doublet at 53.4 ppm (J_{PRh} = 152 Hz), the lack of hydride signals, and the presence of a resonance at δ 9.84 in the ^1H NMR spectrum, which may be reasonably attributed to the coordinated imine hydrogen C*H*═N.

Acknowledgment. The authors thank FONACIT (Venezuela) for financial support to V.L. (financial aid for doctoral studies and Project S3) and B.M. (financial aid for M.Sc. studies), FONACIT and CNR (Italy) for an International Cooperation Grant, the European Community through the MCRTN program AQUACHEM (contract MRTN-CT-2003-503864), and the COST Working Group D17/0003/00 for promoting this scientific activity.

Supporting Information Available: Kinetic data for the hydrogenation of N*β*NA using **1**, **2**, and **3** as catalyst precursors (Tables S1, S2, and S3). This material is available free of charge via the Web at http://pubs.acs.org.

OM0504912